

# We are IntechOpen, the world's leading publisher of Open Access books Built by scientists, for scientists

6,900

Open access books available

186,000

International authors and editors

200M

Downloads

Our authors are among the

154

Countries delivered to

TOP 1%

most cited scientists

12.2%

Contributors from top 500 universities



WEB OF SCIENCE™

Selection of our books indexed in the Book Citation Index  
in Web of Science™ Core Collection (BKCI)

Interested in publishing with us?  
Contact [book.department@intechopen.com](mailto:book.department@intechopen.com)

Numbers displayed above are based on latest data collected.  
For more information visit [www.intechopen.com](http://www.intechopen.com)



# Numerical Investigation of the Shock Train in a Scramjet with the Effects of Back-Pressure and Divergent Angles

*Santhosh Kumar Gugulothu, B. Bhaskar and V.V. Phani Babu*

## Abstract

Numerical simulations are carried out to study the effect of divergence angle and adverse pressure gradient on the movement of shock wave train in a scramjet isolator. The commercial software tool ANSYS Fluent 16 was used to simplify two dimensional Reynolds averaged Navier Stokes equation with compressible fluid flow by considering the density-based solver with standard K- $\epsilon$  turbulence model. The species transport model with single step volumetric reaction mechanism is employed. Initially, the simulated results are validated with experimental results available in open literature. The obtained results show that the variation of the divergence angle and back pressure on the scramjet isolator has greater significance on the flow field. Also, with an increase in the back pressure, due to the intense turbulent combustion, the shock wave train developed should expand along the length and also moves towards the leading edge of the isolator leading to rapid rise in the pressure so that the pressure at the entrance of the isolator can match the enhanced back pressures.

**Keywords:** CFD, scramjet, isolator, divergent angles, back pressure and combustion

## 1. Introduction

The hypersonic air-breathing jet engines are designed to operate in the supersonic-combustion ramjet engine when the Mach number is more than 6. A scramjet engine incorporates with isolator, combustor, and nozzle. Isolator in the scramjet engine is widely used since its inception. Isolator in the scramjet engines is a typical component since it has a significant effect on the dual-mode engine transition. The hypersonic vehicle operates at a particular time during the ascent phase [1]. These effects happen due to the absence of mechanical compressor, free stream air as well as compression ratio. The propulsion vehicle maintained the engine by using inlet and isolator. The main task of the isolator is to differentiate the combustion pressure that occurs in the combustion chamber and should not reach the inlet [2].

Boundary layer interaction observed in the isolator when the dual-mode engine runs with ramjet engine. The air, pressure movement in an isolator, as well as shock

train, are maintained the position of the Mach wave train. The compressed air is adjusted in isolator to match with the condition that can enter into the combustor. When the pressure introduced in the reverse direction of the combustor zone obtained the variation in pressure from the isolator and combustor. The difference between isolator and combustor zone is adjusted by changing the shock wavelength [3]. While designing the isolator, need serious concern about the unstart phenomenon. The isolator may lead to severe effect due to high speed in the flight. The length of the isolator part in the scramjet engine maintains at a certain weight. The required shear and shock waves provided to avoid the communication of the instabilities that will arise and affect the inlet [4]. The system developed using the hypersonic inlet isolator under Mach 4 and Mach 5 flight conditions [5]. In [6], reported that the decrease in the pressure at the inlet of the domain is observed with an increase in the isolator length. The shock train in a fixed 2-D scramjet inlet with isolator showed some results by increasing wall and decreasing the total temperature [7]. In Mach 5 inlet-isolator model, the shock train jumping moments captured by separating flow at the head of the shock train and the contraction ratio of the local throat-like shape [8]. The scramjet isolator decreases the static pressure, and it becomes sharper. The experiment conducted on a constant-area scramjet isolator and observed that was relatively stable with time-resolved and low-frequency pressure [9]. In [10], the numerical simulation influences the movement of free stream characteristics leading to separation with an increase in adverse pressure. The dynamic model of the shock train is predicted on the shock wave layer. The dynamic model cannot suppress the pressure gradient as high as the other sustains [11]. In [12], the complex compression and expansion waves exist in the isolator, causing large stream-wise and transverse gradients upstream of the shock train. The adverse gradient pressure in stream-wise decreases with the duct curvature [13]. In [14], the experiments compared with the conventional approaches using boundary layer interaction large-eddy simulation of a hypersonic of Mach 8 flight vehicle. In [15, 16], they have conducted experiments on the multiple shock wave/turbulent boundary layer interactions in a rectangular duct using Mach numbers 2.45 and 1.6. Carroll et al. observed that the length of the communications and the tendency towards a repeated oblique was scaled directly with the level of confinement. The study of unstart and unstarted flows in an inlet/isolator model strongly associated with boundary-layer separation [17]. The numerical solutions of the Navier-stokes equations for the interactions of a shock wave and turbulent boundary layer varying from 7.93 to 12.17, at a free-stream Mach number of 2.96 and Reynolds number  $1.2 \times 10^7$ . The free-stream predicts accurate results. When shock strength and overall rise pressure for the low viscosity pressure asymptotes. The large-eddy 3-D analysis in the area of uniform cross section with low aspect ratio rectangular duct geometry is studied [18–22].

In the open literature, by varying the adverse pressure gradient at the exit of the isolator the motion path and characteristics of the shock wave train are obtained. In this work, we intend to study the impact of combustion phenomena on shock wave train. Therefore, the significance of the angle of attack on the wall surface of the domain and the effect of the adverse pressure gradient on the movement of the shock wave train are analyzed. The present analysis focused on different divergent angles, i.e., 0, 0.5, 1, and 1.5° with constant pressure gradient of 90 kPa, and also with different negative pressures of 80 and 100 kPa with constant cross-sectional area of the isolator is discussed. All these effects are studied on similar computational domain with similar solver type parameters. The rest of the paper is as organized as follows, Physical model and simulation methodology is discussed in Section 2, the effects of back pressure and angle of attack are discussed in Section 3.

## 2. Physical model, simulation methodology and validation of computational fluid dynamics code

### 2.1 Physical model

In this work, analysis has been carried out on the scramjet isolator of uniform cross section to analyze the movement of shock wave train to study the relation between shock train and the interaction of the boundary layer formation. As shown in **Figure 1** to study the impact of adverse pressure and the significance of divergent angles on the behavior of shock wave train are studied using ANSYS Fluent 16 [23]. The atmospheric air is injected at the entrance of the isolator with 220 mm length and 32 mm height. The hydrogen fuel is injected transversely from the either sides of the wall at a distance of 232.8 mm of the inlet of the computational domain.

### 2.2 Simulation methodology

The commercial software ANSYS Fluent 16 [23] was used to simplify two-dimensional compressible fluid flow by considering the density-based solver with standard K- $\epsilon$  turbulence model, Reynolds-averaged Navier Stokes equation with finite volume method was considered. The species transport model with single step volumetric reaction mechanism is considered to simplify the combustion model (finite rate/eddy dissipation model) [24–27]. To maintain the proper mixing and optimizing the combustion phenomena in supersonic flow RANS approach is the most effective and faster method. The standard K- $\epsilon$  turbulence model is chosen due to its ability of simplifying the negative pressure gradient in the case of transverse injection flow field.

The appropriate governing Eqs. (1)–(5) describing the continuity equation, Navier Stokes equation and combustion model for fluid flow is written as [21, 22, 28, 29].

Continuity equation:

$$\frac{\partial \rho}{\partial t} + \frac{\partial(\rho u_j)}{\partial x_j} = 0 \quad (1)$$

Conservation of momentum (Navier–Stokes equation)

$$\frac{\partial(\rho u_i)}{\partial t} + \frac{\partial(\rho u_i u_j)}{\partial x_j} = -\frac{\partial p}{\partial x_j} + \frac{\partial}{\partial x_j} \left[ \mu_{eff} \left( \frac{\partial u_i}{\partial x_j} + \frac{\partial u_j}{\partial x_i} \right) \right] + S_{ui} \quad (2)$$

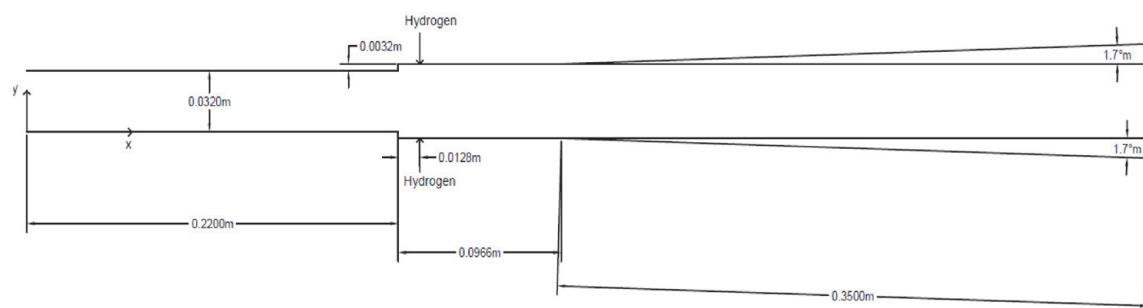


**Figure 1.** Schematic diagram of the scramjet combustor.

where the source term  $S_{ui}$  includes Coriolis and centrifugal forces

$$S_{ui} = -2\Omega \times U - \Omega \times (\Omega \times r)$$

Conservation of energy equation:

$$\frac{\partial(\rho H)}{\partial t} - \frac{\partial \rho}{\partial t} + \frac{\partial(\rho u_i H)}{\partial x_j} = \frac{\partial}{\partial x_j} \left( k \frac{\partial T}{\partial x_j} + \frac{\mu_i}{Pr_i} \frac{\partial h}{\partial x_j} \right) + S_E \quad (3)$$

Turbulence transport equations:

K- $\epsilon$  turbulence model and turbulence eddy dissipation equation

$$\frac{\partial(\rho k)}{\partial t} + \frac{\partial(\rho k u_j)}{\partial x_j} = \frac{\partial}{\partial x_j} \left( \left( \mu + \frac{\mu_t}{\sigma_{k3}} \right) \frac{\partial k}{\partial x_j} \right) + \tau_{ij} \frac{\partial u_i}{\partial x_j} - \beta^* \rho k w \quad (4)$$

$$\frac{\partial \rho \epsilon}{\partial t} + \frac{\partial(\rho u_j \epsilon)}{\partial x_j} = \frac{\partial}{\partial x_j} \left( \Gamma_k \frac{\partial \epsilon}{\partial x_j} \right) + \frac{\epsilon}{k} (C_{\epsilon 1} P_k - \rho C_{\epsilon 2} \epsilon) \quad (5)$$

## 2.3 Combustion modeling

To simulate the combustion flow dynamics more attention is required as rapid turbulence creation and chemical reaction is required. The species transport model with single step volumetric reaction mechanism is considered to simplify the combustion model (finite rate/eddy dissipation model) which is mainly used in the present research work. The global one step chemical reaction of hydrogen combustion has been considered in this paper for its capability of predicting the overall performance parameters with considerably less computational cost for the scramjet combustor. In this global one step reaction mechanism the rate constants like pre-exponential factor (A) and activation temperature are considered as  $9.87 \times 10^8$ . The one step volumetric reaction mechanism is defined as shown in the Eq. (6):



## 2.4 Boundary condition

An atmospheric air is injected at a velocity of 1200 m/s with a hydraulic diameter of 0.05 m and turbulence intensity of 5%. Hydrogen fuel is injected transversely through the either sides of the walls at  $x = 0.220$  m at a velocity of 900 m/s with a turbulence intensity of 5%. No slip condition and constant heat flux is chosen along the solid surface with standard wall function. Interior combustor zone was chosen for the fluid domain (**Table 1**).

Parameters	Hydrogen Jet	Free-stream jet
Mach number [M]	1.0	4.5
Temperature [K]	1000	1300
Pressure [Pa]	506,625	101,325
$C_{H_2}$	1.0	0
$C_{O_2}$	0	0.21
$C_{H_2O}$	0	0.032

**Table 1.**  
Inlet conditions for hydrogen and air jet.

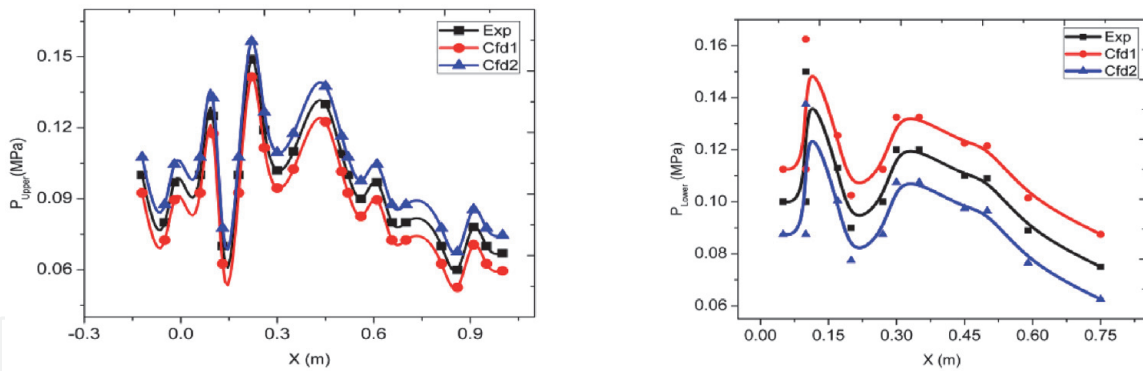


**Figure 2.**  
*Wall pressure distribution at mid-plane and bottom wall of the domain.*

### 2.5 Validation of numerical methods and grid independency

To validate the accuracy of numerical results it is required to compare with the experimental results in order to validate the reliability of computational tool. Computational results predominantly depend on the quality of the mesh and size; therefore, it is also necessary to find out the ideal grid size. Initially, computational analysis is carried out to validate the commercial code and simultaneously find out the ideal grid size by considering 634,846 (CFD1, fine mesh) and 384,592 (CFD2, coarse mesh) [25]. The obtained simulated results (**Figure 2**) are then validated by with the experimental data [25] available in open literature and found to be in good qualitative agreement. It is observed that simulation which own fine grid and coarse grid has a good accuracy that the relative error is below 5%. Therefore, the CFD tool can be applied to capture the shock wave reasonably well in terms of both location and strength of the shock wave system [25].

### 3. Results and discussions

In the present study, the significance of the angle of attack on the wall surface of the domain and the effect of the adverse pressure gradient on the movement of the shock wave train are analyzed. The present analysis focused on different divergent angles, i.e., 0, 0.5, 1 and 1.5° with a standard pressure gradient of 90 kPa, and also with different negative pressures of 80 and 100 kPa with constant cross-sectional area of the isolator is discussed.

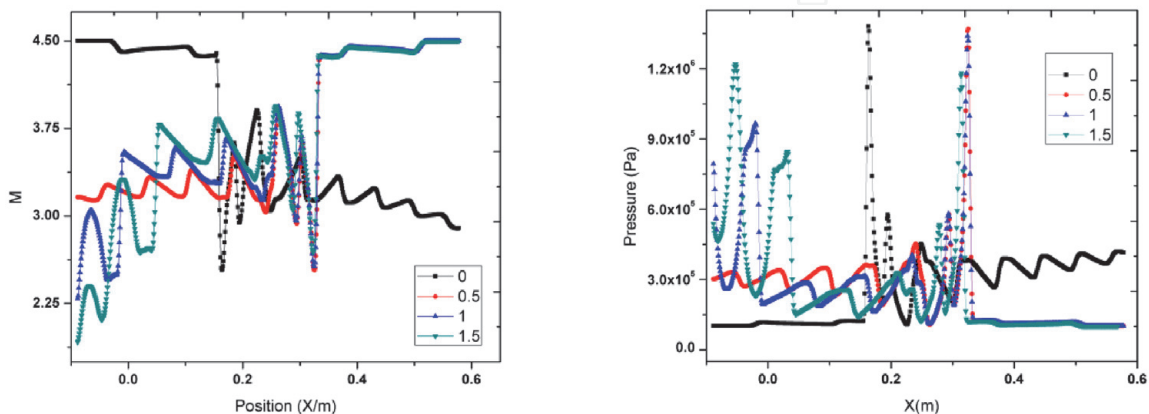


**Figure 3.**  
*Mach number and pressure variation along the mid-plane.*

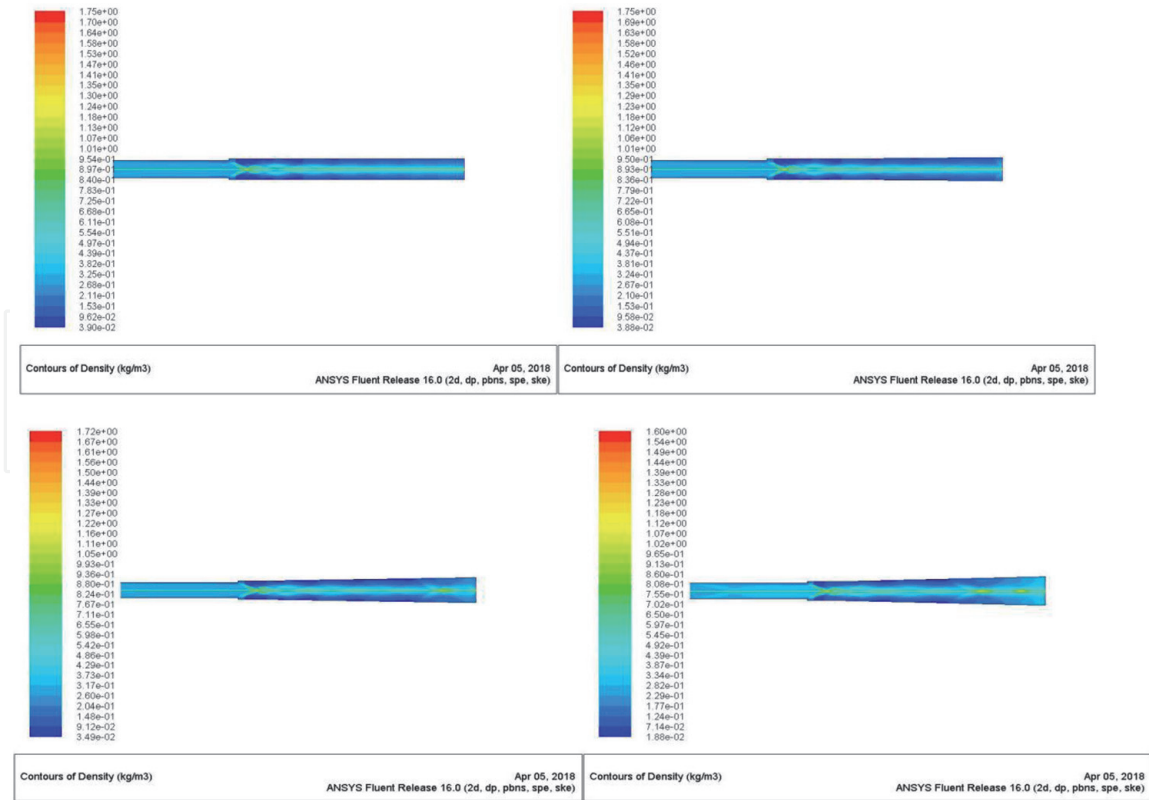


**Figure 4.**  
Density distribution at constant back pressure with variable divergence angles.

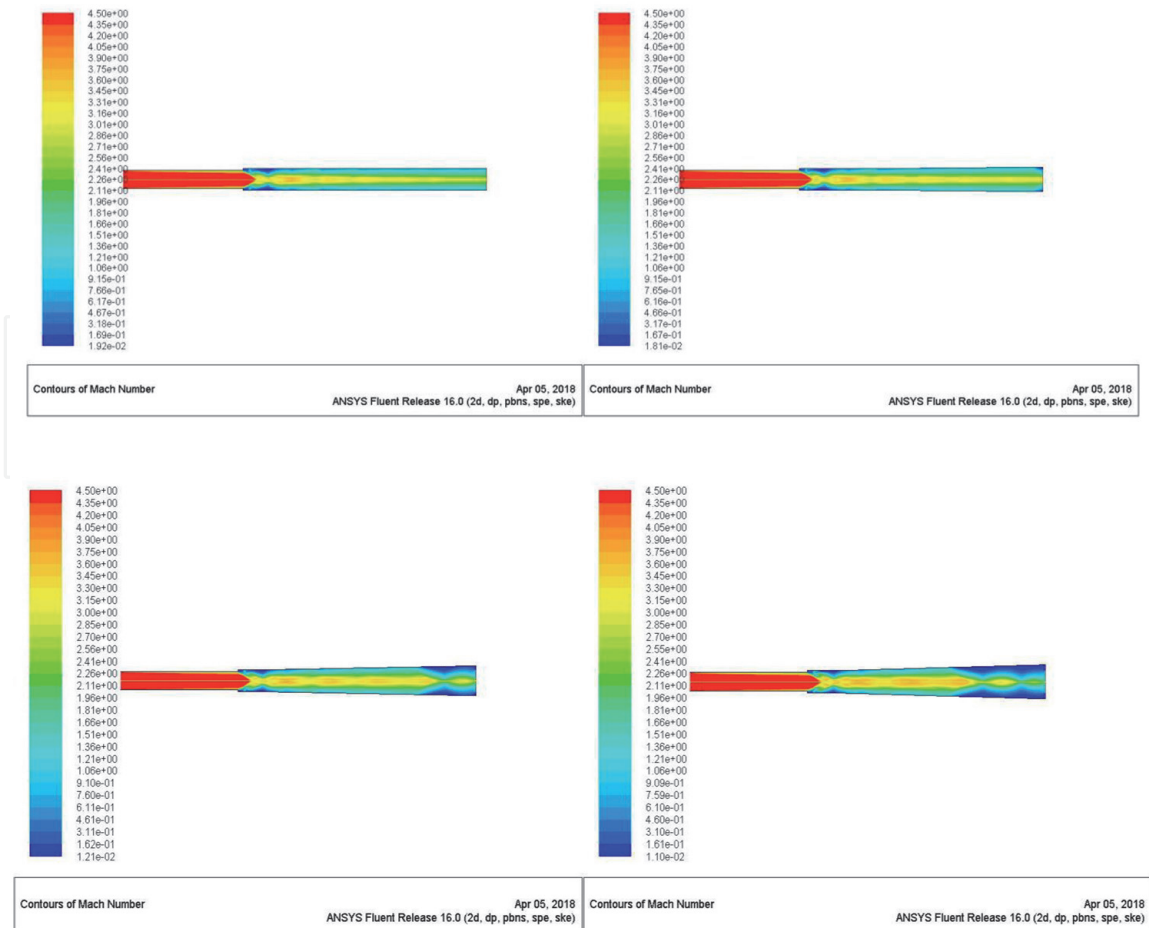


**Figure 5.**  
Mach distribution at constant back pressure with variable divergence angles.

### 3.1 Impact of divergent angles

In this work, analysis has been carried out at a standard back pressure of 90 kPa with different divergent angles, i.e., 0, 0.5, 1 and 1.5° are considered. The basic purpose of considering the different divergent angles is to analyze the movement of the combustion phenomena inside the isolator. For each divergent angle with a standard adverse pressure gradient of 90 kPa, the contour lines of static temperature, mass density, Mach number and static pressure are measured. From **Figures 3–7**, it is observed that with an increase in the divergent angle the location of the shock train will be moved near the leading edge of the domain. At a divergent angle of 1.5°, as the flow gets separated the strong expansion wave is generated leading to negative pressure drop at the inception of the Mach wave train. When compared to the divergent angles of 1 and 1.5° in the scramjet isolator, the divergent angle of 0° with constant isolator area supports better back pressure. This is because with an increase in the divergence angle, the shock train generated inside the isolator converts the Mach shock wave into normal shock wave initially and again converts into oblique shock wave. The drawbacks of the normal shock wave generated inside the isolator due to an increase in the divergent angle leads to boundary layer separation on the either sides of the wall of the domain, resulting in the decrease of the intensity of the initial shock wave train. **Figure 3** represents the Mach number and static pressure distribution along the axis of the isolator with different divergent angles. From **Figures 3–7** it is noted that variation in divergence angle leads to stronger shock wave train resulting in rapid pressure losses. The

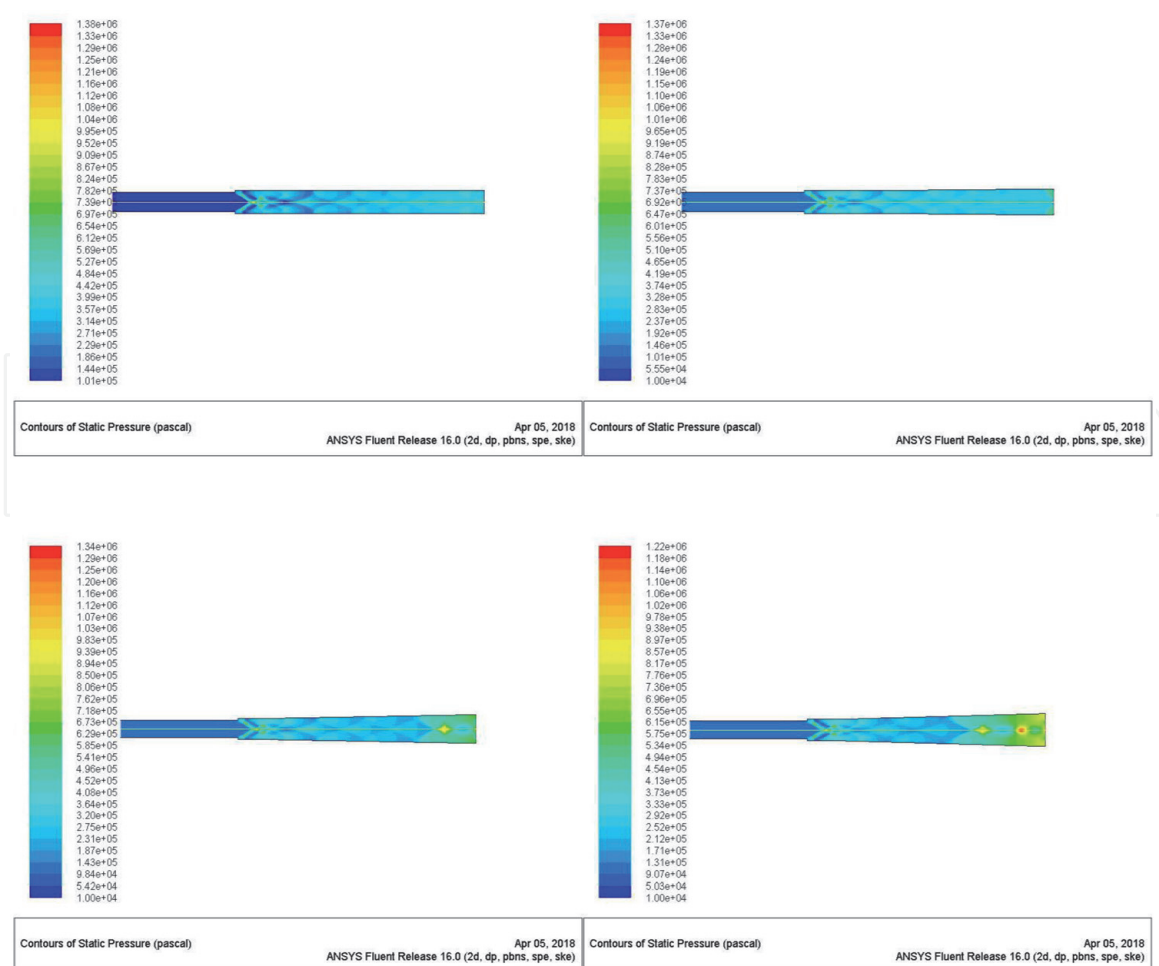


**Figure 6.** Static pressure distribution at constant back pressure with variable divergence angles.

impact of the divergent angle on the scramjet combustor has greater significance on the flow field.

### 3.2 Variation of the back pressures

In the present analysis, the effect of back pressure (i.e., 80, 90 and 100 kPa) on the performance of the domain with uniform cross-sectional area (i.e., divergent angle of  $1.5^\circ$ ) are studied. The back pressure of 80 and 100 kPa are identified based on the experimental results by Sun et al. **Figures 8–11** represent the contour lines of static pressure, density, Mach number and temperature along the Mid-plane with

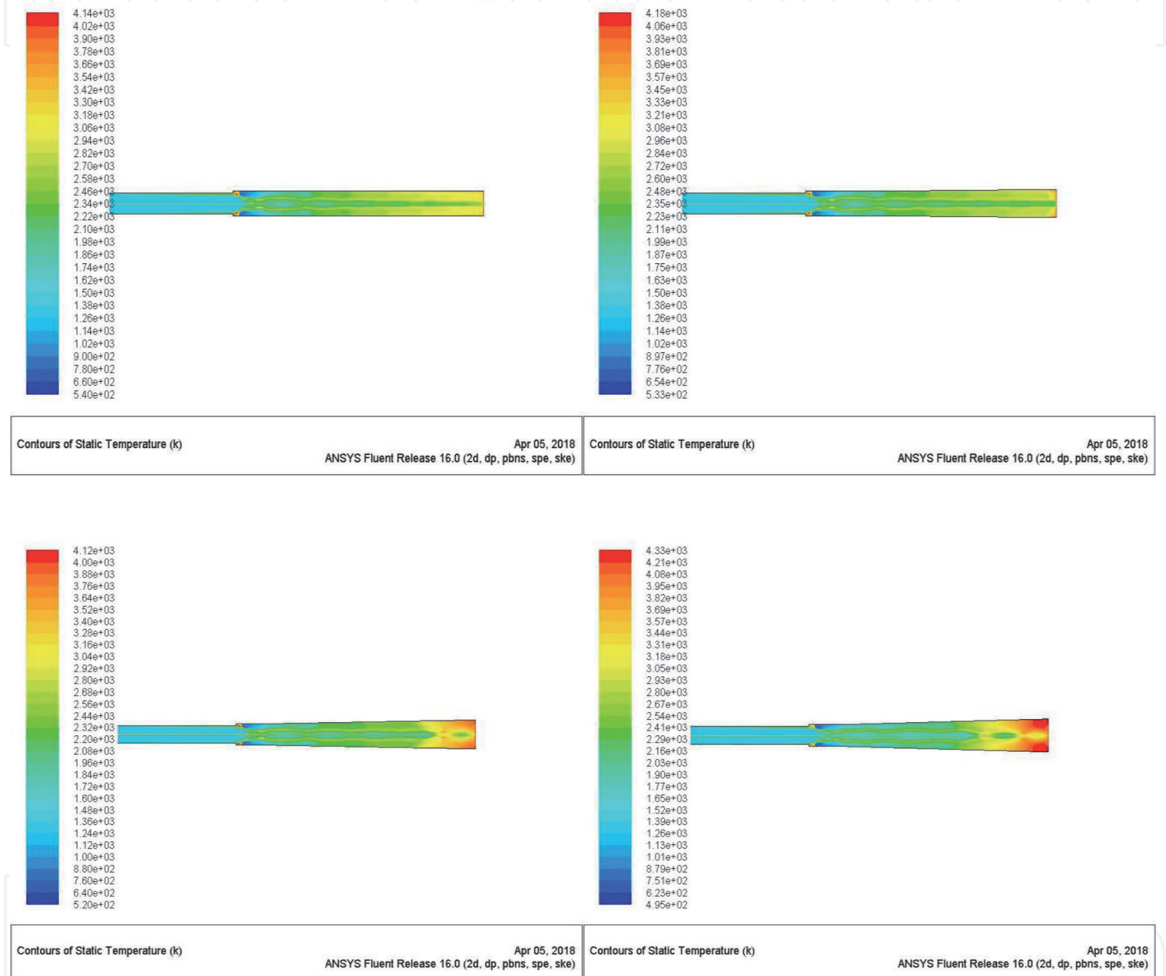


**Figure 7.** Static pressure distribution at constant back pressure with variable divergence angles.

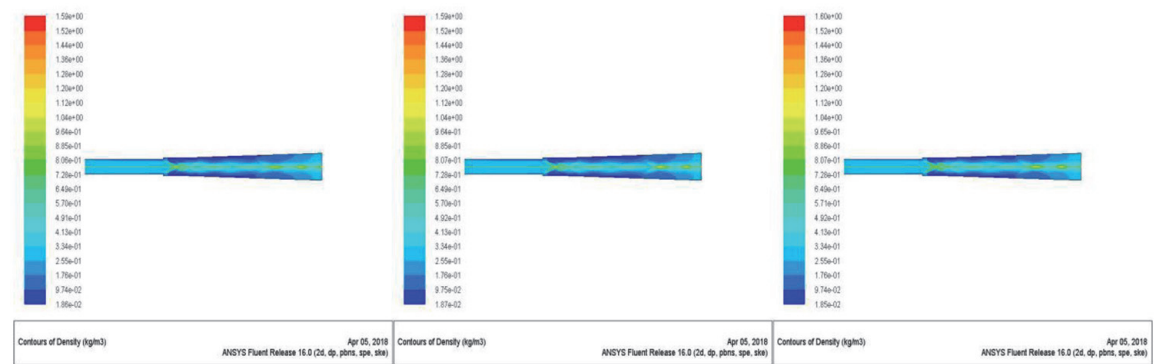


**Figure 8.** Density distribution with uniform cross-sectional area with different back pressure.

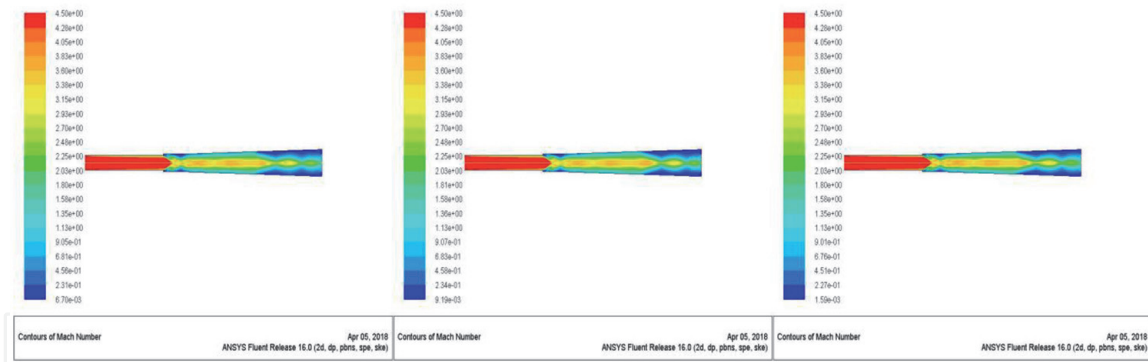


**Figure 9.**  
 Mach number distribution with uniform cross-sectional area with different back pressure.

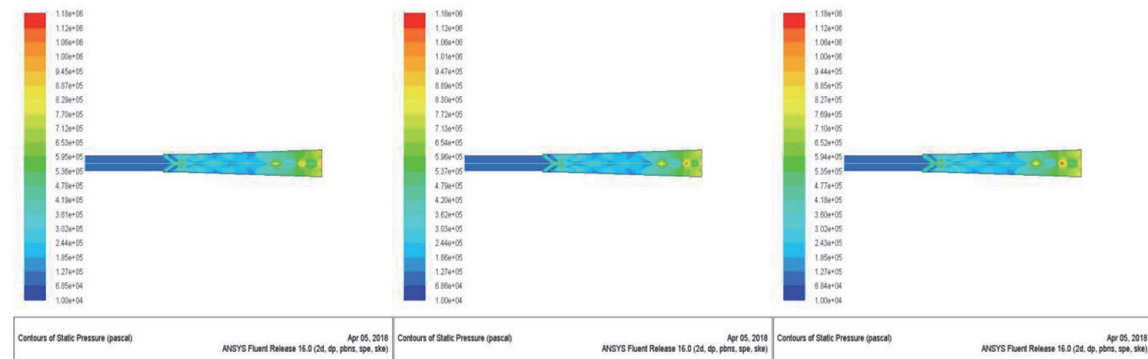


**Figure 10.**  
 Static pressure distribution with uniform cross-sectional area with different back pressure.

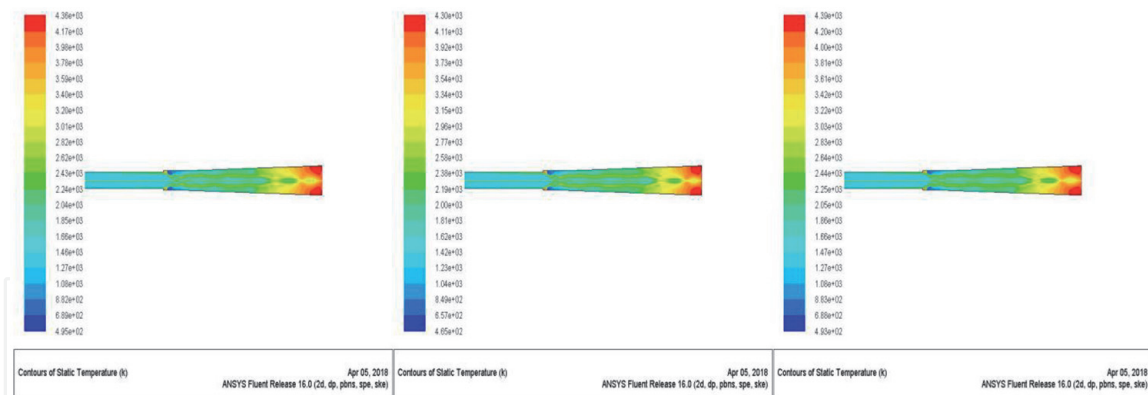


**Figure 11.**  
 Static temperature distribution with uniform cross-sectional area with different back pressure.

different back pressure at a uniform cross-sectional area. From the results, it is noted that with an increase in the adverse pressure due to the rapid mixing of the fluid particles, the shock wave train developed lead to intense combustion, the Mach train developed should expand along the length and also moves towards the leading edge of the isolator leading to rapid rise in the pressure along the axis of the isolator so that the pressure at the inlet of the isolator can match the enhanced negative pressure. Additionally, as the shock wave train approaches the supersonic inlet, the unstart conditions are observed at the entrance of the isolator. A strong separation region occurs because of the interaction between shock wave and boundary layer. Due to the increase in the pressure gradient four Mach disks are observed in the domain. With different back pressure of 80, 90 and 100 kPa, symmetric planes of the scramjet isolator the contours of the static temperature,

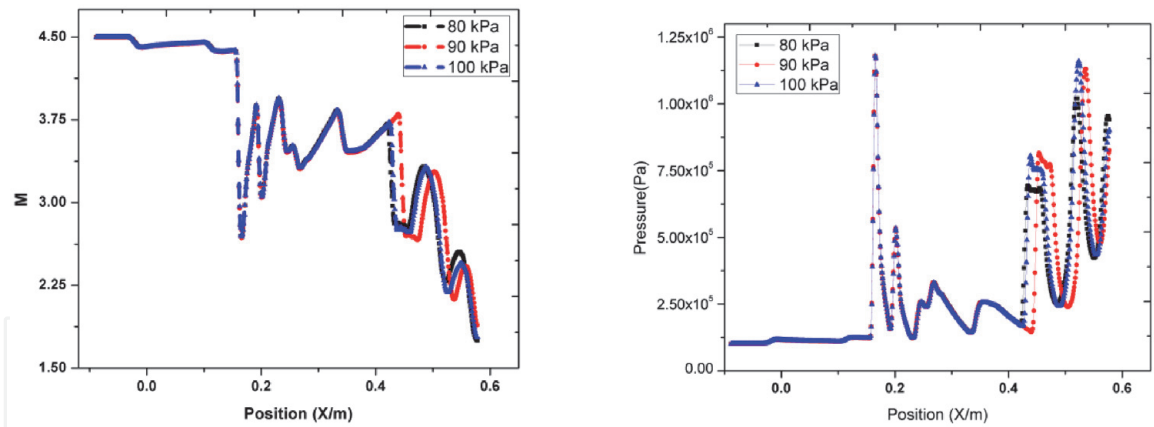


**Figure 12.** Mach number and pressure variation along the mid-plane with different back pressure at a uniform cross-sectional area.

pressure, Mach number and density are shown in the figure. From the results it is observed that at a back pressure of 80 kPa in the scramjet isolator, enhancement in pressure is affected due to the presence of the normal or oblique shock waves. Whereas in the case of 90 kPa back pressure, pressure rise is noted far away from the shock wave train due to the intermixing of the disorganized streamlines developed by the shock wave train. Additionally, when compared to downstream mixing region additional enhancement in the static pressure is observed due to the development of upstream shock wave train. For an adverse pressure of 100 kPa, the pressure drops in a given length due to fanno flow is much higher when compared to the increase in pressure due to intermixing and also the peak pressure is observed followed by the sequential reduction in pressure.

From **Figure 12**, it is observed that the static pressure along the axis of the isolator is observed to increase substantially. Also, with different back pressure investigated it is observed that the static pressure distribution does not get influenced significantly because of the Mach wave train in the shock wave region of the isolators.

#### 4. Discussions

The present analysis is focused on the significance of diverging angles and the effect of adverse pressure gradient on the behavior of the shock wave train is analyzed using the simulation. An identical flow inlet is considered at the inception point of the scramjet isolator for different diverging angles, i.e., 0, 0.5, 1 and 1.5° followed by different back pressure, i.e., 80, 90 and 100 kPa have been investigated. The following has been observed. It is observed that the shock wave train has moved near to the leading edge of the isolator with an increase in the divergent angle. At a divergent angle of 1.5°, as the flow gets separated the strong expansion wave is generated leading to the negative pressure drop at the inception of the shock wave train. When compared to the divergent angles of 1 and 1.5° in the scramjet isolator, the divergent angle of 0° with constant isolator area supports better back pressure. With an increase in adverse pressure gradient, because of the intense turbulent combustion, the shock wave train developed should expand along the length and also moves towards the leading edge of the isolator leading to rapid rise in the pressure so that the pressure at the inlet of the domain can match the enhanced negative pressure. A strong separation region occurs because of the interaction between shock wave and boundary layer.

# IntechOpen

## Author details

Santhosh Kumar Gugulothu<sup>1\*</sup>, B. Bhaskar<sup>2</sup> and V.V. Phani Babu<sup>3</sup>

<sup>1</sup> Department of Mechanical Engineering, National Institute of Technology, Andhra Pradesh, India

<sup>2</sup> Department of Mechanical Engineering, GITAM School of Technology, Hyderabad, India

<sup>3</sup> Department of Mechanical Engineering, MLR Institute of Technology, Hyderabad, India

\*Address all correspondence to: [santoshgk1988@gmail.com](mailto:santoshgk1988@gmail.com)

## IntechOpen

---

© 2020 The Author(s). Licensee IntechOpen. This chapter is distributed under the terms of the Creative Commons Attribution License (<http://creativecommons.org/licenses/by/3.0>), which permits unrestricted use, distribution, and reproduction in any medium, provided the original work is properly cited. 

## References

- [1] Xu K, Chang J, Li N, Zhou W, Daren Y. Experimental investigation of mechanism and limits for shock train rapid forward movement. *Experimental Thermal and Fluid Science*. 2018;**98**: 336-345
- [2] Xu K, Chang J, Zhou W, Daren Y. Mechanism of shock train rapid motion induced by variation of attack angle. *Acta Astronautica*. 2017;**140**:18-26
- [3] Chen Z, Yi SH, Ahmed NA, Kong XP, Quan PC. Transient behavior of shock train with and without controlling. *Experimental Thermal and Fluid Science*. 2015;**66**:79-96
- [4] Huang W, Wang Z-G, Pourkashanian M, Ma L, Ingham DB, Luo S-B, et al. Numerical investigation on the shock wave transition in a three-dimensional scramjet isolator. *Acta Astronautica*. 2011;**68**(11-12):1669-1675
- [5] Reinartz BU, Herrmann CD, Ballmann J, Koschel WW. Aerodynamic performance analysis of a hypersonic inlet isolator using computation and experiment. *Journal of Propulsion and Power*. 2003;**19**(5):868-875
- [6] Balu G, Panneerselvam S, Rathakrishnan E. Computational studies on the performance of an isolator for a dual mode scramjet engine. *International Journal of Turbo and Jet Engines*. 2005;**22**(4):255-264
- [7] Fischer C, Olivier H. Experimental investigation of the shock train in an isolator of a scramjet inlet. In: 17th AIAA International Space Planes and Hypersonic Systems and Technologies Conference; 2011. p. 2220
- [8] Le DB, Goyne CP, Krauss RH, McDaniel JC. Experimental study of a dual-mode scramjet isolator. *Journal of Propulsion and Power*. 2008;**24**(5): 1050-1057
- [9] Xu K, Chang J, Li N, Zhou W, Daren Y. Preliminary investigation of limits of shock train jumps in a hypersonic inlet-isolator. *European Journal of Mechanics - B/Fluids*. 2018; **72**:664-675
- [10] Tan HJ, Sun S, Huang HX. Behavior of shock trains in a hypersonic inlet/isolator model with complex background waves. *Experiments in Fluids*. 2012;**53**(6):1647-1661
- [11] Huang H-x, Tan H-j, Sun S, Wang Z-y. Behavior of shock train in curved isolators with complex background waves. *AIAA Journal*. 2017:329-341
- [12] Krishnan L, Sandham ND, Steelant J. Shock-wave/boundary-layer interactions in a model scramjet intake. *AIAA Journal*. 2009;**47**(7):1680-1691
- [13] Carroll BF, Dutton JC. Characteristics of multiple shock wave/turbulent boundary-layer interactions in rectangular ducts. *Journal of Propulsion and Power*. 1990;**6**(2):186-193
- [14] Wagner JL, Yuceil KB, Valdivia A, Clemens NT, Dolling DS. Experimental investigation of unstart in an inlet/isolator model in Mach 5 flow. *AIAA Journal*. 2009;**47**(6):1528-1542
- [15] Xu K, Chang J, Zhou W, Yu D. Mechanism and prediction for occurrence of shock train sharp forward movement. In: 51st AIAA/SAE/ASEE Joint Propulsion Conference; 2015. p. 3747
- [16] Li N, Chang J-T, Xu K-J, Yu D-R, Bao W, Song Y-P. Prediction dynamic model of shock train with complex background waves. *Physics of Fluids*. 2017;**29**(11):116103
- [17] Erdem E, Kontis K, Johnstone E, Murray NP, Steelant J. Experiments on

- transitional shock wave–boundary layer interactions at Mach 5. *Experiments in Fluids*. 2013;**54**(10):1598
- [18] Geerts J, Yu K. Experimental characterization of isolator shock train propagation. In: 18th AIAA/3AF International Space Planes and Hypersonic Systems and Technologies Conference; 2012. p. 5891
- [19] Koo H, Raman V. Large-eddy simulation of a supersonic inlet-isolator. *AIAA Journal*. 2012;**50**(7):1596-1613
- [20] Shang JS, Hankey WL Jr, Law C. Numerical simulation of shock wave-turbulent boundary-layer interaction. *AIAA Journal*. 1976;**14**(10):1451-1457
- [21] Morgan B, Duraisamy K, Lele SK. Large-eddy simulations of a normal shock train in a constant-area isolator. *AIAA Journal*. 2014;**52**(3):539-558
- [22] Versteeg HK, Malalasekera W. *An Introduction to Computational Fluid Dynamics: The Finite Volume Method*. England: Pearson Education; 2007
- [23] Fluent Inc. *Guide, FLUENT User's. Version 6.2.16*. Lebanon, New Hampshire: Fluent Inc.; 2005
- [24] Gugulothu SK. Significance of fluid flow characteristics in the hydrogen-fuelled scramjet combustor using flame stabilisation analysis. *Australian Journal of Mechanical Engineering*. 2019;**2**:1-10
- [25] Gugulothu SK, Nutakki PK. Dynamic fluid flow characteristics in the hydrogen-fuelled scramjet combustor with transverse fuel injection. *Case Studies in Thermal Engineering*. 2019;**14**:100448
- [26] Gugulothu SK. A systematic literature review based on different fuel injection strategies used in scramjet combustors. *Heat Transfer - Asian Research*
- [27] Dharavath M, Manna P, Sinha PK, Chakraborty D. Numerical analysis of a kerosene-fueled scramjet combustor. *Journal of Thermal Science and Engineering Applications*. 2016;**8**(1): 011003
- [28] Huang W, Liu W-d, Li S-b, Xia Z-x, Liu J, Wang Z-g. Influences of the turbulence model and the slot width on the transverse slot injection flow field in supersonic flows. *Acta Astronautica*. 2012;**73**:1-9
- [29] Soni RK, Ashoke D. Investigation of strut-ramp injector in a Scramjet combustor: Effect of strut geometry, fuel and jet diameter on mixing characteristics. *Journal of Mechanical Science and Technology*. 2017;**31**(3): 1169-1179